Assessment of material-atmosphere interactions during scanning laser cleaning of archaeological bronze alloys: A Roman coin case study

Lasers in the Conservation of Artworks XIII – Siano & Ciofini (eds)

Assessment of material-atmosphere interactions during scanning laser cleaning of archaeological bronze alloys: A Roman coin case study

E. Di Francia & S. Grassini
Dipartimento di Scienza Applicata e Tecnologia (DISAT), Politecnico di Torino, Torino, Italy

D. Neff
NIMBE/LAPA-IRAMAT, CEA/CNRS/Université Paris-Saclay, UMR3685, CEA Saclay, Gif/Yvette, France

R. Lahoz
Instituto de Nanociencia y Materiales de Aragón, (INMA), CSIC - Universidad de Zaragoza, Zaragoza, Spain

ABSTRACT: The main goal of this research was to assess the presence of possible re-oxidation phenomena during laser cleaning procedures carried out on Cu-based archaeological artefacts. Previous studies conducted on archaeological and artificial corrosion layers, highlighted that the laser ablation procedures (removal of unwanted materials) do not change the composition of the corrosion layers and that detectable re-oxidation phenomena occur on laser-treated surfaces for intense laser conditions, not applicable on Cultural Heritage artefacts. A novel approach, recently developed on Material Science field by these Authors, is here applied in the Conservation Science field: the use of a traceable isotope combined with Time-of-Flight Secondary Ion Mass Spectrometry (ToF-SIMS) on an archaeological bronze coin. This approach, applied for the first time on an archaeological artefact, allows assessing the presence of possible re-oxidation phenomena that might occur on object surfaces during optimised cleaning procedures.

1 INTRODUCTION

In recent years, many researches have been focused on laser applications on a wide range of artefacts (Landucci et al. 2000, Siano et al. 2012). Despite the very good performance of laser cleaning, the complex phenomena that take place during laser-material interaction are usually very difficult to describe. Nevertheless, very few systematic studies have been reported on the effects of the laser cleaning on highly heterogeneous materials such as Cu-based metal alloys. Generally they have been focused on discussions of laser-interaction mechanisms, chemical characterisation of laser effects on surfaces (Bertasa & Korenberg 2022; Di Francia et al. 2021), or systematic studies of the laser parameters to be applied on metal artefacts (Burmester et al. 2005, Di Francia et al. 2018, 2022). Indeed, knowing the laser-material interactions in depth will help to optimise the laser cleaning parameters and make it a more efficient procedure.

In addition to this, the complex stratified structure of the corrosion products grown on the Cu-based archaeological artefacts buried in soil should be considered, as model by Robbiola in a two-layer or a three-layer structure. In the two-layer model, a protective copper oxide layer (*noble* patina) grows in contact with the metal and then several types of unwanted, corrosion products might grow on it. These unwanted corrosion products are inhomogeneous

DOI: 10.1201/9781003386872-27

and polycrystalline structures which might differ in composition (due to oxygen, humidity and soil elements, e.g. Si, Fe, Ca), and so in their chemical and physical properties. Furthermore, these products can also degrade, transforming the cuprous products into cupric products and incorporating soil elements, forming new compounds as e.g. brochantite ($Cu_4(OH)_6(SO)_4$) and malachite ($Cu_2(OH)_2CO_3$). In the three-layer model, dangerous and reactive corrosion products form due to the presence of Cl^- ions in the environment: the Cl^- ions penetrate trough both the external porous layer of Cu(II) compounds (e.g. hydroxysilicates, hydroxyphosphates, hydroxychlorides) and the middle layer of cuprite (Cu_2O) up to the internal copper oxide layer, in contact with the metal. This concentration of Cl^- ions, at the metal-corrosion interface, can activate the formation of reactive cuprous chlorides (nantokite, CuCl), starting a cyclical and dangerous copper corrosion process, commonly noun as *bronze disease* (Robbiola et al. 1998, Soffritti et al. 2014).

The nature of these inhomogeneous and polycrystalline structures should be taken in consideration during the ablation process: indeed, the laser energy interacts with the material decaying into heat and generating a stress wave, which can cause disaggregation of the constituents and creation of reactive radicals. As a consequence, it is possible to assist at the formation of a plasma plume composed by free species (multiphoton/thermionic ionizations) of the ablated materials and the surrounding environment, forming a cloud (plume) on the treated surface. Eventually, if the substrate melts, it is possible to observe recombination reactions that latter might form by-products (Fotakis et al. 2007). A final parameter of paramount importance that poses an important role in a laser cleaning process is the surrounding atmosphere. Although most of the tests are usually performed in air, there are other works that have tested the cleaning conditions under controlled atmospheres (Gomes et al. 2018, Grigor'eva et al. 2017), to enhance the cleaning efficiency or prevent unexpected reactions on the surface, but never with the aim of studying the laser interaction mechanisms in the presence of a controlled atmosphere.

Due to the complexity of these interactions, several previous laser-cleaning tests had been conducted by our group on artificially-corroded layers simulating the protective patina to be preserved and the unwanted corrosion products to be removed. From these previous works, no changes had been detected in the chemical and microstructural composition of the laser-treated artificially-corroded layers (Di Francia et al. 2018, 2022). Our previous analyses also highlighted that high irradiance values and long pulse duration may cause a re-oxidation phenomenon on the surface during the ablation process. This demonstrated that, even if the composition found after the laser processes is the same, the corrosion compounds might be of new formation (Di Francia et al. 2021).

This work exposes the results obtained applying, for the first time on Cultural Heritage, the already explained procedure for detecting material-atmosphere recombination in controlled synthetic air (Di Francia et al. 2021). Details of the internal and complex stratified corrosion structures of the archaeological coin and of the optimal laser parameters assessment that allows the most effective ablation have been described in previous papers (Di Francia et al. 2018, 2022). The novelty here is that the present work assesses the laser-surface material interactions and, for the first time, the possible presence of re-oxidation phenomena during optimal laser-cleaning treatment conditions on archaeological bronze coin fragments. To achieve this goal, scanning laser experiments have been carried out in a controlled atmosphere enriched with ^{18}O isotope. Then, advanced Time-of-Flight Secondary Ion Mass Spectrometry (ToF-SIMS) analyses have provided the data necessary to detect the possible presence of re-oxidation phenomena.

2 MATERIALS AND METHODS

2.1 *Archaeological samples and their preparation*

The laser-cleaning procedure had been validated on real ancient samples with low archaeological value, a coin (*Follis Massenzio*, Roman Empire bronze coin) coming from a private collection. An extensive description of the coin and the sample preparation before and immediately after the cleaning treatments in synthetic air are reported in (Di Francia et al. 2021, 2022).

2.2 *Laser system and laser parameters*

The laser used for the treatments is a 1064 nm Nd:YAG fibre laser (model EasyMark-20 from Jeanologia). The system works in a Q-Switched (QS) regime, from 4 ns to 200 ns of pulse duration, which pulses are delivered by means of two-galvanic mirrors and are focused with a f-Theta lens with 160 mm of focal distance for a final beam diameter of ca. 30 μm. The laser system is coupled via computer with EzCAD 2.1 UNI, a vector graphic editor, with a CAD-*like* capability that enables users to perform, in a repeatable way, rapid, precise and complex surface scanning treatments.

Two values of energy were chosen for the laser treatments. Those values were optimised in previous works as the energy values suitable for the laser cleaning without damaging the substrate (Di Francia et al. 2018, 2022). Table 1 reports the optimised laser experimental parameters set as a function of the chemical composition of the corrosion products to be removed and applied on different coin fragments.

Table 1. Laser experimental parameters used on the archaeological samples. P (Power), F (Fluence), I (Irradiance), t_p (Pulse Duration), v_{scan} (Scanning Speed) and d_L (Interlining).

Laser parameters					Geometrical parameters	
Test	P (W)	F (J/cm^2)	I (GW/cm^2)	t_p (ns)	v_{scan} (mm/s)	d_L (mm)
1	0.23	1.63	0.41	4	300	0.015
2	0.73	5.16	1.29	4	300	0.015

2.3 *Experimental set-up and assessment of the ablation mechanism on archaeological samples*

The innovative procedure here reported has been already described in (Di Francia et al. 2021) for the assessment of the laser-surface material interaction mechanisms during ablation processes conducted with intense laser conditions on artificially corroded layers. Those conditions were selected to stress possible re-oxidation phenomena.

To assess if a re-oxidation phenomenon occurs during the ablation process, and so if the compounds analysed after the cleaning treatment are the same with the one previously present or they are compounds of new formation, the optimised laser cleaning treatments were performed in a controlled atmosphere chamber filled with synthetic air (20% ^{18}O + 80% N_2). This synthetic air is characterised by the absence of the ^{16}O, the most common oxygen isotope in the natural air: in this way, if re-oxidation phenomena occur, they will be traced by the mostly presence of the ^{18}O in the new compounds and detected by ToF-SIMS analyses (Figure 1).

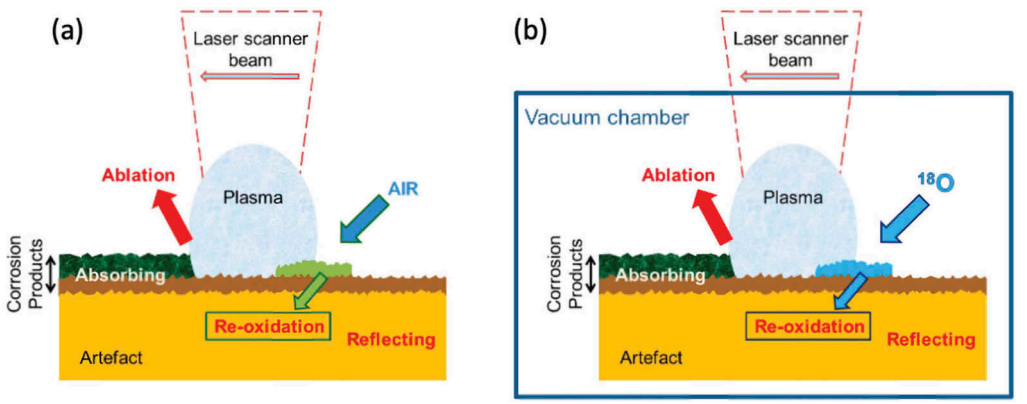

Figure 1. Scheme of laser-cleaning ablation model for Cu-based archaeological artefacts. *a)* Laser-cleaning in natural air *(left)*: possible re-oxidised products (*light green* in the figure) non-detectable; *b)* novel experimental set-up adopted using ^{18}O isotope *(right)*: possible re-oxidised products (*light blue*) detectable.

Laser cleaning tests were conducted positioning the coin fragments in a chamber presenting a window transparent to the infrared radiation. A depression of around 1 bar was done and then the chamber was filled back to recover 1 bar with synthetic air marked by the presence of ^{18}O isotope, an oxygen isotope presents in small amount in natural air, and so in every material (0.205(14) at.%) (Lide 2005).

Moreover, a coin fragment was laser-treated with Test 1 parameters in natural air and then analysed with ToF-SIMS in order to have a control sample.

2.4 *Sample characterisation*

The cross-sections of the non-treated and laser-treated coin samples were characterised by Optical Microscopy (Olympus BX51 microscope equipped with a Nikon EOS camera). It allows to acquire images in Bright and in Dark-Field modality (OM-BF and DF, respectively).

ToF-SIMS analysis (TOF-SIMS 5 instrument from IONTOF) was used to detect percentage amount of ^{18}O isotope on the ablated corrosion product layers of the coin samples; this analysis was performed on both the control sample, treated in natural air, and on the samples treated in synthetic air.

The high sensibility of the ToF-SIMS technique allows detecting very small fractions of the isotope that would be incorporated due to the laser interaction within the synthetic air atmosphere, enriched with the ^{18}O isotope. This will determine how the laser interaction occurs and how the recombination or re-oxidation processes take place.

The sample laser-treated in natural air (Test 1), considered as the control sample, was analysed on two randomly selected areas while on the samples irradiated in synthetic air, in the conditions of Test 1 and Test 2, were respectively acquired two and three random selected areas. Subsequently, for each selected area, the isotopic oxygen ratio percentage (O_r) was calculated as follows:

$$O_r = \frac{^{18}O}{^{18}O + ^{16}O} * 100 \tag{1}$$

where O_r is the isotopic oxygen ratio percentage; ^{18}O is the isotopic amount of ^{18}O; ^{16}O is the isotopic amount of ^{16}O.

Two sources of uncertainty, strictly connected with the applied measurement parameters, were also considered for each acquisition, as previously reported (Di Francia et al. 2021).

The arithmetic mean values obtained were used as the O_r estimation, while type-B uncertainties (u_B) were used to characterise the measurements. The type-B uncertainty was estimated according to the count number of the ^{18}O measurements.

The data and the results here presented are in accordance with the *Guide to the Expression of Uncertainty in Measurement* (GUM 2008).

3 RESULTS

3.1 *Cross-section analysis and composition of the laser-cleaned archaeological corrosion products*

Extensive discussion of the results are present in previous works (Di Francia et al. 2018, 2022), however here is extremely important to report that OM observations on the non-treated cross-section coin fragment had showed the presence of an outer corrosion products layer (*external* and *intermediate* layers) completely corroded, up to 200 μm-in thickness, and an internal and partially corroded layer, up to 800 μm-in thickness (Figure 2). From the picture, the heterogeneity in composition of the outer layer is shown by the presence of a *lighter grey* layer (intermediate layer) between the internal and the *darker grey* external corrosion products layers. The figure schematises also the structure.

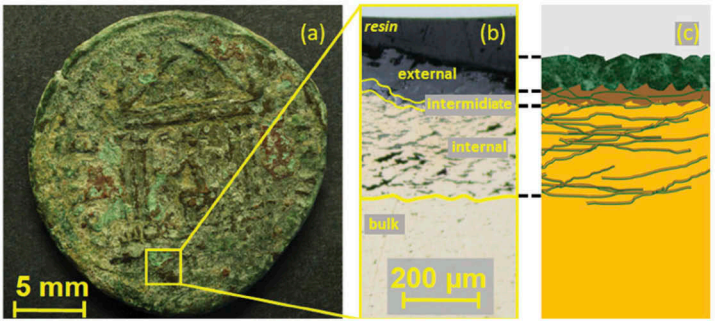

Figure 2. High-resolution coin photograph and OM cross-section image of the Roman Empire coin: verso side of the coin (left), cross-section acquired by optical microscope, bright field (centre) and scheme of the internal structure (right).

Deeper, Figure 3 compares the DF-OM observations of the cross-sections, for both laser-treated samples (Test 1 and Test 2), with the non-treated one. These analyses showed the complex nature of archaeological stratified corrosion products. Indeed the coin presented a turquoise green colouration (Cu^{++} compounds, e.g. hydroxychloride, hydroxycarbonates) overlapped to a thinner red-brown-in colour layer (Cu^{+} compounds, e.g. cuprous oxide) with spot-areas where only red-brown colouration was presented; yellowish-in colour (possible cuprous chloride or a mix of copper and nanometric tin oxides) areas or very thin layers were presented between the green and the red-brown layers (Soffritti et al. 2014, Robbiola et al. 1998). The Figure 3 shows that this structure was still present on both laser-treated samples: no qualitative differences in the composition of the outer corrosion products on the non-treated and the laser-treated samples were detectable.

Both laser treatments removed part of the corrosion products: Test 2 (I, 1.29 GW/cm^2) reduced the outer (external and intermediate) corrosion layer, in average, up to ≈41 µm while for Test 1 (I, 0.41 GW/cm^2) only a marginal average thickness reduction up to ≈15 µm was observed. Moreover, the laser probable interacted only with the surface of the outer corrosion products layers without reaching the internal layer and the artefact metal: at the highest value in irradiance (Test 2), the laser interacted with and partially ablated the external Cu^{++} and the intermediate Cu^{+} compounds layers. Due to a more compactness and thickness of the archaeological corrosion layers compared to the artificially-corroded ones, Test 2 resulted more efficient in terms of ablation of archaeological corrosion products respect to the optimal laser conditions discussed in (Di Francia et al., 2018).

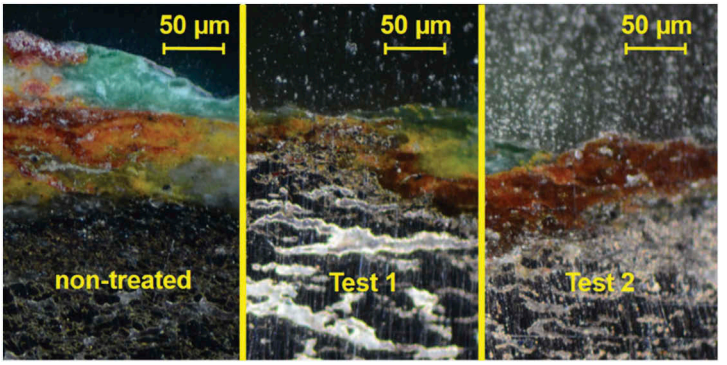

Figure 3. DF-OM observations of the cross-sections: comparison of the non-treated, Test 1 and Test 2 samples.

3.2 *ToF-SIMS identification of isotope incorporation*

ToF-SIMS maps supported the identification of an internal corrosion layer, in the shape as a net (characterised by the presence of chlorine isotopes), overlapped by a more corroded outer layer (identified by the presence of oxygen and copper isotopes). The structure was still present after the higher irradiance values of Test 2, as Figure 4 shows. The presence of chlorine in the internal layer, Cu^{+} in the intermediate layer and Cu^{++} in the external layer, might suggest the interaction of the coin with an aggressive burial environment (Robbiola et al. 1998).

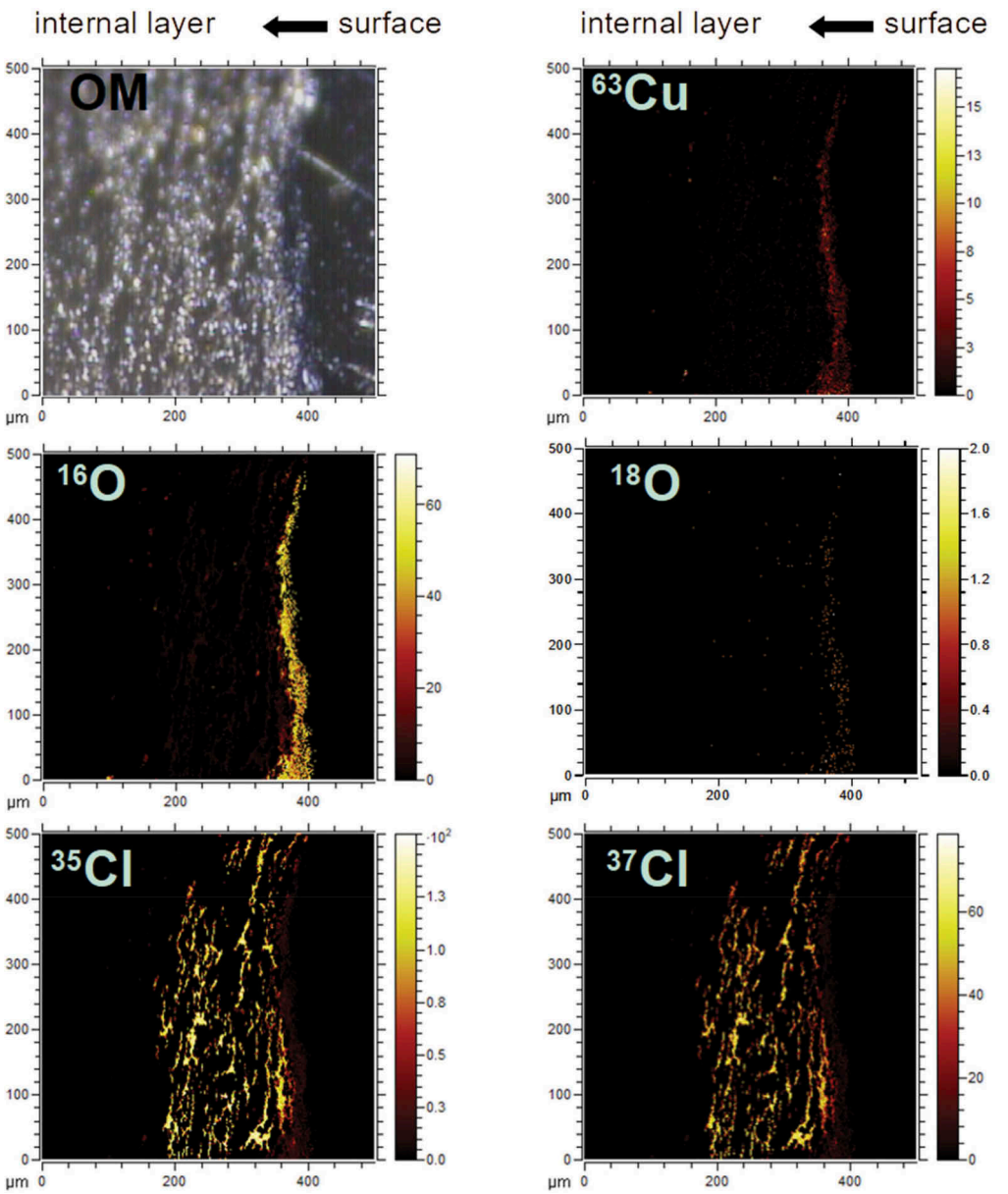

Figure 4. Stratifications of the corrosion layers: OM image (up left) and example of ToF-SIMS maps of different isotopes on Test 2-area cross-section.

4 DISCUSSION AND ASSESSMENT OF THE LASER-SURFACE MATERIAL INTERACTIONS DURING LASER ABLATION ON ARCHAEOLOGICAL SAMPLES

To assess if the optimised laser-cleaning parameters can induce surface re-oxidation phenomena on real corrosion product layers, several areas on the cross-section samples were considered: two areas of the cross-section controlling sample and, respectively, two and three areas of the cross-section samples treated in the chamber filled with synthetic air.

Table 2 shows the obtained figures of isotopic oxygen ratio percentage (O_r) and the corresponding type-B uncertainties (u_B) for each sample.

Table 2. O_r and u_B determined on the Follis Massenzio coin fragments laser-treated in natural and synthetic air with laser Test 1 parameters and Test 2 parameters.

Laser Test	Air	O_r *average*	u_B
1	natural	0.212	0.006
1	synthetic	0.218	0.007
2	synthetic	0.233	0.009

As said previously, Test 2 presents the best cleaning results on the coin and, as expected, this test has also the highest content of O_r, as shown in Table 2.

The data showed that the O_r of the controlling sample (and so of the coin) is close to the ^{18}O% natural abundance of (0.205(14) at.%), as reported in (Lide, 2005): during the laser treatment, if re-oxidation occurred, the interaction would took place with the isotopes in the amounts of the natural air, so no differences would be observed with respect to the non-treated coin and to the natural isotope abundance.

Different the case of both laser-treated coin fragments in synthetic air: a possible increase of isotope ratios as a function of the irradiance values can be hypothesised. However, for Test 1 (I, 0.41 W/cm^2), laser-treated in synthetic air, knowing that the ^{18}O% natural abundance value percentage is (0.205(14) at.%), it was not possible to assess the presence of re-oxidation phenomena since the O_r average values (0.218%) is in the range of the ^{18}O% natural abundance uncertainty. Whereas for Test 2 (I, 1.29 GW/cm^2), laser-treated in synthetic air, the O_r average value (0.233%) is slightly above this range, at the limit of reliability to detect difference in abnormal amount of ^{18}O%.

Even though that, this kind of interaction was not excluded: it is possible that with these irradiance values, a re-oxidation occurred but in a very little amount.

This can be explained by the too low irradiance values of Test 1 and Test 2 used in this study, that lead to an insufficient interaction with the synthetic air, to be clearly detected by ToF-SIMS analyses. For both Tests, it can also be explained by a dilution effect: if laser induces re-oxidation phenomena, they occur at the surface layer (with a different depth penetration in dependence of the corrosion products present). Analysing the cross-sections, the *region of interest* selected probably had interacted with the synthetic air but, however, it is possible that part of the information come from an area not touched by the re-oxidation phenomenon.

In fact, at this pulse duration and irradiance values, the laser energy interacted with the heterogeneous corrosion layers, partially ablating them. The reactive radicals and the free electrons of the ablated material present either in the plasma or on the laser-treated surface might have interacted with the oxygen present in the atmosphere.

Even if, in synthetic air, slight differences of O_r averages of Test 1 and Test 2 were detected respect to ^{18}O% natural abundance (0.205(14) at.%), it is highly probable that they are not due to normal fluctuation of the ratio: a re-oxidation trend is detectable at the increase of the irradiance values (Di Francia et al. 2021).

These optimised parameters probably generate re-oxidation phenomena but, in any case, in a little amount, barely outside the uncertainty value of the ^{18}O natural abundance (0.205(14) at.%).

5 CONCLUSIONS

The results here presented confirm the need of validating the optimised condition acquired on artificially-corroded samples on real archaeological corrosion products, due to their complexity in inhomogeneous and polycrystalline structure. Moreover, the use of a scanning laser system allows performing, in a repeatable way, surface homogeneous treatments.

In this work, an innovative approach was introduced, for the first time in the Conservation Field, in order to assess if a re-oxidation on the ablated surfaces occur during the laser cleaning of an archaeological Cu-based artefact by a NIR Q-switched Nd:YAG fibre laser.

ToF-SIMS technique applied on the archaeological artefact samples, treated in ^{18}O traced atmosphere, revealed an isotopic oxygen ratio percentage at the limit of reliability to detect difference in abnormal amount of ^{18}O%. Nevertheless, even if the detected amounts are slight above the range of the ^{18}O % natural abundance uncertainty, an interaction of the corrosion product layers with the air during the laser treatments was determined.

This validation experiment demonstrates that it is highly probable that re-oxidation phenomena occur even with the optimised laser-cleaning parameters used in conservation, as it may find reported with the applied laser-cleaning parameters used in other cleaning processes (Di Francia et al. 2021).

To conclude, at the optimised laser-cleaning conditions for archaeological corrosion products, re-oxidation phenomena would occur in a very slight amount. Therefore, at those laser conditions, laser-cleaning procedure can be considered as a low-invasive cleaning procedure which does not significantly modify the treated layers.

Laser-cleaning operators in the conservation field may find useful to know about this possible re-oxidation so they can keep attention especially on heterogeneous materials, where each point can behave in a different way towards the same combination of laser parameters.

ACKNOWLEDGEMENTS

The Authors would like to thanks the European Federation of Corrosion (EFC) for supporting the measurement campaign in the frame of the EUROCORR Young Scientist Grant 2016 and Dr Jacopo Corsi for donating the bronze coin. The author R. Lahoz wishes to acknowledge professional support of the CSIC Interdisciplinary Thematic Platform "Open Heritage: Research and Society (PTI-PAIS)".

FUNDING

This work was partially supported by the European Federation of Corrosion (EFC) [EUROCORR Young Scientist Grant 2016].

REFERENCES

Bertasa, M. & Korenberg, C. 2022. Successes and challenges in laser cleaning metal artefacts: A review. *J Cult Herit* 53:100–17. https://doi.org/10.1016/j.culher.2021.10.010.

Burmester, T., Meier, M., Haferkamp, H., Barcikowski, S., Bunte, J. & Ostendorf, A. 2005. Femtosecond Laser Cleaning of Metallic Cultural Heritage and Antique Artworks. In Dickmann K, Fotakis C, Asmus JF (eds) *Lasers Conserv. Artworks. Springer Proc. Physics, vol 100*. Berlin, Heidelberg: Springer. https://doi.org/10.1007/3-540-27176-7_8.

Fotakis, C., Anglos, D., Zafiropulos, V., Georgiou, S. & Tornari, V. 2007. *Lasers in the Preservation of Cultural Heritage: Principles and Applications* (Series in Optics and Optoelectronics). CRC Press.

Di Francia, E., Lahoz, R., Neff, D., Angelini, E. & Grassini, S. 2018. Laser cleaning of Cu-based artefacts: Laser/corrosion products interaction. *Acta IMEKO* 7. https://doi.org/10.21014/acta_imeko.v7i3.610.

Di Francia, E., Lahoz, R., Neff, D., de Caro, T., Angelini, E. & Grassini, S. 2022. Laser-cleaning effects induced on different types of bronze archaeological corrosion products: chemical-physical surface characterisation. *Appl Surf Sci* 573:150884. https://doi.org/10.1016/j.apsusc.2021.150884.

Di Francia E., Lahoz R., Neff D., Rico V., Nuns N., Angelini E. 2021. Novel procedure for studying laser-surface material interactions during scanning laser ablation cleaning processes on Cu-based alloys. *Appl Surf Sci* 544:148820. https://doi.org/10.1016/j.apsusc.

Gomes, V., Dionísio, A., Pozo-Antonio, J.S., Rivas, T. & Ramil, A. 2018. Mechanical and laser cleaning of spray graffiti paints on a granite subjected to a SO_2-rich atmosphere. *Construction and Building Materials* 188(10): 621–632.

Grigor'eva, I.A., Parfenov, V.A., Prokuratov, D.S. & Shakhmin, A.L. 2017. Laser cleaning of copper in air and nitrogen atmospheres. *Journal of Optical Technology* 84(1): 1–4.

Guide to the Expression of Uncertainty in Measurement (GUM). Int Bur Weight Meas n.d. https://www.bipm.org/en/ publications/guides/gum.html.

Landucci, F., Pini, R., Siano, S., Salimbeni. R. & Pecchioni. E. 2000. Laser cleaning of fossil vertebrates: A preliminary report. *Journal of Cultural Heritage* 1(Suppl. 1): S263–S267. https://www.sciencedirect.com/science/article/pii/S1296207400001412

Lide, D.R. 2005. CRC *Handbook of Chemistry and Physics*, Internet Version https://doi.org/10.1016/0165-9936(91)85111-4.

Robbiola, L., Blengino, J.M., Fiaud, C. 1998. Morphology and mechanisms of formation of natural patinas on archaeological Cu-Sn alloys. *Corrosion Science* 40: 2083–2111.

Siano, S., Agresti, J., Cacciari, I., Ciofini, D., Mascalchi, M., Osticioli, I. & Mencaglia, A.A. 2012. Laser cleaning in conservation of stone, metal, and painted artifacts: State of the art and new insights on the use of the Nd:YAG lasers. *Applied Physics A Mater Sci Process* 106: 419–46. https://link.springer.com/article/10.1007/s00339-011-6690-8.

Soffritti, C., Fabbri, E., Merlin, M., Garagnani, G.L. & Monticelli, C. 2014. On the degradation factors of an archaeological bronze bowl belonging to a private collection. *Applied Surface Science* 313:762–70. https://www.sciencedirect.com/science/article/pii/S016943321401352X.